Original Article
Mol Imaging Radionucl Ther 2021;30:177-186 DOI:10.4274/mirt.galenos.2021.25633

Relationships Between DCE-MRI, DWI, and ^{18}F-FDG PET/CT Parameters with Tumor Grade and Stage in Patients with Head and Neck Squamous Cell Carcinoma

Baş Boyun Yassı Hücreli Kanser Hastalarında Tümör Derecesi ve Evre ile DK-MRG, DAG ve ^{18}F-FDG PET/BT Parametrelerinin İlişkisi

Hande Melike Bülbül[1], Ogün Bülbül[2], Sülen Sarıoğlu[3], Özhan Özdoğan[4], Ersoy Doğan[5], Nuri Karabay[6]

[1]*Recep Tayyip Erdoğan Training and Research Hospital, Clinic of Radiology, Rize, Turkey*
[2] *Recep Tayyip Erdoğan Training and Research Hospital, Clinic of Nuclear Medicine, Rize, Türkiye*
[3]*Dokuz Eylül University Faculty of Medicine, Department of Medical Pathology, İzmir, Turkey*
[4]*Dokuz Eylül University Faculty of Medicine, Department of Nuclear Medicine, İzmir, Turkey*
[5]*Dokuz Eylül University Faculty of Medicine, Department of Otorhinolaryngology, İzmir, Turkey*
[6]*Dokuz Eylül University Faculty of Medicine, Department of Radiology, İzmir, Turkey*

Abstract

Objectives: Properties of head and neck squamous cell carcinoma (HNSCC) such as cellularity, vascularity, and glucose metabolism interact with each other. This study aimed to investigate the associations between diffusion-weighted imaging (DWI), dynamic contrast-enhanced magnetic resonance imaging (DCE-MRI), and positron emission tomography/computed tomography (PET/CT) in patients with HNSCC.

Methods: Fourteen patients who were diagnosed with HNSCC were investigated using DCE-MRI, DCE, and ^{18}fluoride-fluorodeoxyglucose PET/CT and evaluated retrospectively. Ktrans, Kep, Ve, and initial area under the curve (iAUC) parameters from DCE-MRI, ADC_{max}, ADC_{mean}, and ADC_{min} parameters from DWI, and maximum standardized uptake value (SUV_{max}), SUV_{mean}, metabolic tumor volume (MTV), and total lesion glycolysis (TLG) parameters from PET were obtained. Spearman's correlation coefficient was used to analyze associations between these parameters. In addition, these parameters were grouped according to tumor grade and T and N stages, and the difference between the groups was evaluated using the Mann-Whitney U test.

Results: Correlations at varying degrees were observed in the parameters investigated. ADC_{mean} moderately correlated with Ve ($p=0.035$; $r=0.566$). Ktrans inversely correlated with SUV_{max} ($p=0.017$; $r=-0.626$). iAUC inversely correlated with SUV_{max}, SUV_{mean}, TLG, and MTV ($p<0.05$, $r\leq-0.700$). MTV (40% threshold) was significantly higher in T4 tumors than in T1-3 tumors ($p=0.020$). No significant difference was found in the grouping made according to tumor grade and N stage in terms of these parameters.

Conclusion: Tumor cellularity, vascular permeability, and glucose metabolism had significant correlations at different degrees. Furthermore, MTV may be useful in predicting T4 tumors.

Keywords: Cancer of the head and neck, squamous cell carcinoma, diffusion, permeability, positron emission tomography

Öz

Amaç: Baş boyun yassı hücreli karsinomunun (BBYHK) hücresellik, vaskülarite ve glukoz metabolizması gibi özellikleri birbirleri ile etkileşim içerisindedir. Bu çalışmanın amacı BBYHK hastalarında difüzyon ağırlıklı görüntüleme (DAG), dinamik kontrastlı manyetik rezonans görüntüleme (DK-MRG) ve pozitron emisyon tomografisi/bilgisayarlı tomografi (PET/BT) arasındaki ilişkinin araştırılmasıdır.

Address for Correspondence: Hande Melike Bülbül MD, Recep Tayyip Erdoğan Training and Research Hospital, Clinic of Radiology, Rize, Turkey
Phone: +90 506 938 93 94 **E-mail:** handemelikehalac@gmail.com ORCID ID: orcid.org/0000-0001-9492-093X
Received: 15.05.2021 **Accepted:** 19.07.2021

©Copyright 2021 by Turkish Society of Nuclear Medicine
Molecular Imaging and Radionuclide Therapy published by Galenos Yayınevi.

Yöntem: BBYHK tanısı almış ve DAG, DK-MRG ve ^{18}flor-florodeoksiglukoz (^{18}F-FDG) ile görüntüleme yapılmış 14 hasta retrospektif olarak değerlendirildi. DK-MRG'den Ktrans, Kep, Ve iAUC; DAG'den ADC_{maks}, ADC_{mean} and ADC_{min} ve ^{18}F-FDG PET/BT'den SUV_{maks}, SUV_{mean}, metabolik tümör hacmi (MTV) and toplam lezyon glikolizi (TLG) parametreleri elde edildi. Bu parametreler arasındaki ilişki Spearman korelasyon katsayısı kullanılarak değerlendirildi. Ayrıca bu parametreler tümör derecesi, T ve N evresine göre gruplandırılarak gruplar arasındaki ilişki Mann-Whitney U testi kullanılarak analiz edildi.

Bulgular: İncelenen parametreler arasında değişen düzeylerde korelasyonlar gözlendi. ADC_{mean} ve Ve arasında orta düzeyde pozitif korelasyon saptandı (p=0,035; r=0,566). Ktrans ile SUV_{maks}'ın negatif korelasyon gösterdiği (p=0,017; r=-0,626), iAUC ile SUV_{maks}, SUV_{mean}, TLG ve MTV arasında negatif yönde güçlü korelasyon olduğu gözlendi (p<0,05, r≤-0,700). MTV (%40 x SUV_{maks} eşik değer) T4 tümörlerde T1-3 tümörlere kıyasla istatistiksel olarak anlamlı düzeyde yüksekti (p=0,020). Tümör derecesi ve N evresine göre yapılan gruplamada parametreler arasında anlamlı fark saptanmadı.

Sonuç: Tümörün hücreselliği, vasküler permeabilite ve glukoz metabolizması farklı derecelerde anlamlı korelasyonlar gösterdi. Ayrıca, MTV değeri T4 tümörleri tahmin etmede faydalı olabilir.

Anahtar kelimeler: Baş boyun kanseri, yassı hücreli kanser, difüzyon, pozitron emisyon tomografisi, permeabilite

Introduction

Head and neck cancers constitute 4-5% of all malignancies. Among these, head and neck squamous cell carcinoma (HNSCC) constitutes the thumping majority with 90% (1).

Although magnetic resonance imaging (MRI) and computed tomography (CT) are indispensable for diagnosis and follow-up, functional imaging techniques such as dynamic contrast-enhanced (DCE) MRI, diffusion-weighted imaging (DWI), and positron emission tomography (PET)/CT are adjunctive modalities that give information about the underlying biology (2,3).

^{18}Fluoride-fluorodeoxyglucose (^{18}F-FDG) PET/CT is a modality with high sensitivity in the diagnosis of primary tumors and has been used for staging tumors, evaluating treatment responses, and identifying HNSCC recurrence (4,5). Besides ^{18}F-FDG PET/CT parameters like standardized uptake values (SUVs), total lesion glycolysis (TLG), and metabolic tumor volume (MTV) are important biomarkers of tumor behavior (5,6). For example, MTV and TLG are prognostic predictors of non-small cell lung cancers (NSCLC) and head and neck cancers (7,8). They are also valuable for predicting tumor responses to neoadjuvant chemotherapy in breast cancer, NSCLC, and osteosarcomas (9,10,11).

DCE-MRI and DWI are helpful methods for the characterization of the pathophysiological features of tumors (12,13). DWI provides quantitative information about tumor cellularity, and this is expressed by the apparent diffusion coefficient (ADC). DCE-MRI allows the determination of values such as tumor-vascular permeability and extracellular-extravascular volume fraction with quantitative parameters obtained by pharmacokinetic modeling by imaging the signal change with the administration of contrast agent (14).

Accordingly, DWI, DCE-MRI, and ^{18}F-FDG PET/CT can provide supplementary information about biological properties such as cellularity, metabolic activity, and angiogenesis in HNSCC (1,14).

Many multiparametric investigations were conducted including these modalities to clarify the complicated biology of HNSCC (2,3). But results were discordant. Although some authors have reported correlations between ADC and PET parameters (15,16), some did not show a correlation among them (17,18). The same discrepancy is found for the correlation between DCE-MRI and PET parameters and tumor grade in different studies (2,3,6).

Properties of tumor tissues such as cellularity, vascularity, and glucose metabolism interact with each other. It is essential to define this relationship because it can be valuable for clinical practice in predicting the tumor treatment response and locoregional recurrence and evaluating the treatment response in different tumor groups (19,20).

This study aimed to analyze associations between ^{18}F-FDG PET/CT, DWI, and DCE-MRI in patients with HNSCC.

Material and Methods

Dokuz Eylül University Institutional Ethics Board approved this study (file number: 5538-GOA). Because of its retrospective design, the necessity for written informed consent was waived.

Patients

The hospital database was used to identify patients with HNSCC between January 2018 and September 2019. The inclusion criteria were as follows: 1) Patients with HNSCC and histopathological diagnosis and 2) patients who underwent routine imaging work-up including DCE-MRI, DWI sequences, and ^{18}F-FDG PET/CT. The exclusion criteria were the following: 1) inadequate MRI images due to severe artifacts (n=1), 2) tumor treatment before MRI and ^{18}F-FDG PET/CT, 3) patients whose ^{18}F-FDG PET/CT images are ineligible for evaluation due to attenuation, and 4) MRI or ^{18}F-FDG PET/CT images that were obtained

at another hospital (n=4). After these criteria, 14 patients were included in this study.

Eight patients had a biopsy, and six had both a biopsy and an excision. MRI examinations were conducted before tissue samples were collected (average 4 days, range: 1-7 days). The mean time interval between biopsy and ^{18}F-FDG PET/CT examinations was 10 days (range: 7-15 days). A pathologist with 28 years of experience in head and neck cancer examined the specimens obtained at these procedures. The cases were divided into two groups based on the T stage, where patients in T1, T2, and T3 stages were included in group 1 (n=8) and those in T4 stages in group 2 (n=6). We divided the patients into two groups as those with (n=8) and without (n=6) lymph node metastases. For statistical purposes, all oropharyngeal carcinomas associated with HPV and well and moderately differentiated squamous cell carcinomas were grouped as low grade (n=10), whereas non-keratinizing undifferentiated laryngeal carcinomas and poorly differentiated squamous cell carcinomas were grouped as high grade (n=4).

MRI Examinations

MRI was performed for all patients using a 1.5 T MR scanner (Achieva, Philips Medical Systems, Netherlands) with an 8-channel head and neck array coil. The standard MRI protocols included axial T2-weighted (T2W) turbo spin-echo (TSE), axial and sagittal T1-weighted (T1W) spin-echo, coronal short-tau ınversion-recovery TSE, and axial, sagittal, and coronal fat-suppressed contrast-enhanced T1W TSE (spectral presaturation with ınversion recovery).

DWI was performed using an axial echo planar imaging DWI sequence (b0 and b800 s/mm^2). DWI parameters were as follows: TR/TE, 10165/111; matrix, 204×230; slice thickness, 5 mm; cross-section spacing, 0 mm. ADC maps were automatically generated by the implemented software.

DCE imaging was performed using the T1W DCE sequences (T1W single-shot turbo field echo). T1 map was calculated with two flip angles of 5° and 15° (TR: 10 ms and TE: 2.4 ms, axial plane, section thickness: 3 mm) before the DCE-MRI sequence. T1W DCE sequence was acquired with the following parameters: TR, 5 ms; TE, 2.4 ms; FOV, 220×220 mm; matrix, 140×114; flip angle, 258; slice thickness, 5 mm; 26 slices, NEX, 1.5; 50 dynamic cycles; total acquisition time, 5 min 36 s. Gadoterate meglumine was injected at a dose of 0.2 mmol/kg and at the rate of 2 mL/s, intravenously with an automatic injector, and then, 20 mL saline was injected.

Analysis of the DCE-MRI and DWI Images

One radiologist under the supervision of a senior radiologist with 6 and 11 years of experience in head and neck oncology, respectively, analyzed the DWI and DCE-MRI images. All images were transferred to a software module (IntelliSpace Portal-v8.2.20820, Philips Medical Systems), and all measurements were conducted using the workstation.

The ADC value was measured on ADC maps by drawing the region of interest (ROI) on the tumor at the level of its largest diameter that was explained previously (1). T1W and T2W MR images were used while drawing the ROI to avoid the necrotic and hemorrhagic components of the tumor. ADC_{max}, ADC_{mean}, and ADC_{min} parameters were measured using this method (Figure 1).

ROIs were manually drawn in the tumor on DCE images in the same way that explained for the ADC analysis. Tofts model was used to calculate pharmacokinetic parameters in every case according to the population-averaged arterial input function (21). The parameters were as follows:

Ktrans, volume transfer constant;

Ve, volume of the extravascular extracellular leakage space (EES);

Kep, redistribution rate constant (Kep = Ktrans × Ve^{-1});

iAUC, initial area under the curve.

^{18}F-FDG PET/CT Examinations

Whole-body ^{18}F-FDG PET/CT was performed using a combined PET/CT scanner (Philips Gemini TOF, 16 Slices). After 6-h fasting, 0.11 mCi/kg ^{18}F-FDG was injected intravenously if blood sugar was <200 mg/dL. All patients rested for an hour in a quiet and no lightroom, and then, PET/CT scanning was performed from the vertex to the upper thigh (1.5 min/bed).

SUV_{max}, SUV_{mean}, MTV, and TLG were calculated using freely available software LIFEx (version 6.3, lifexsoft.org) (22). The highest SUV in the given volume of interest (VOI) is called SUV_{max}. The average SUV of the VOI is called SUV_{mean}. MTV is a measurement of metabolically active tumor volume according to ^{18}F-FDG avidity. TLG is calculated by multiplying MTV by SUV_{mean}.

Analysis of the ^{18}F-FDG PET/CT Images

One nuclear medicine physician analyzed ^{18}F-FDG PET/CT images under the supervision of a senior nuclear medicine physician with 5 and 12 years of experience in ^{18}F-FDG PET/CT imaging for head and neck cancer, respectively. A VOI was placed around the primary tumor area in correlation with MRI, including all hypermetabolic tumor areas, excluding physiological uptake areas such as palatine

tonsils and mylohyoid muscle. For MTV, the following two methods were used: fixed absolute threshold by SUV 2.5 and fixed relative threshold by 40% of SUV_{max}. TLG was also determined using these two methods (23,24) (Figure 1).

Statistical Analysis

Descriptive statistics were presented as mean, standard deviation, median, and range. Shapiro-Wilks test was conducted to determine the distribution of normality of all data. Spearman's correlation coefficient was used to analyze the associations between investigated parameters. The Mann-Whitney U test was performed to analyze the association between DCE-MRI, DWI, and ^{18}F-FDG PET/CT with the group of grade and T stage. Receiver operating characteristics (ROC) analysis was conducted to determine the ability of MTV data to distinguish advanced-stage tumors.

All statistical analyses were performed using the SPSS version 24 software (SPSS Inc, Chicago, IL, USA). The $p<0.05$ was considered statistically significant in all analyses.

Results

Patients

All patients were male with a median age of 58 years, range 38-78 years. Lesion localization was oral cavity in 5 (35.7%) patients, larynx in 5 (35.7%), oropharynx in 2 (14.3%), and nasopharynx in 2 (14.3%). The T stages of tumor were T1 in 3 (21.4%), T2 in 3 (21.4%), T3 in 2 (14.3%), and T4 in 6 (42.9%) of patients. Of tumors, 10 (71.4%) were low grade, and 4 (28.6%) were high.

Imaging

A complete summary of the results, including mean values, standard deviation, median, and ranges, is shown in Table 1.

It was determined that in overall measurements, ADC_{mean} moderately correlated with Ve ($p=0.035$; $r=0.566$; Table 2). Ktrans inversely correlated with SUV_{max} ($p=0.017$; $r=-0.626$; Table 3). There was a strong inverse correlation of iAUC with SUV_{max}, SUV_{mean}, TLG, and MTV (both 40% and SUV 2.5 threshold; $p=0.00$; $r=-0.732$; $p=0.005$; $r=-0.700$, $p=0.002$; $r=-0.745$, $p=0.000$; $r=-0.824$, $p=0.000$; $r=-0.815$, $p=0.000$; $r=-0.815$, respectively). In addition, there was a tendency to inverse correlation between SUV_{max} and ADC_{mean}, but it was not statistically significant ($p=0.053$, $r=-0.526$).

There was no significant correlation between other parameters of DCE, DWI, and ^{18}F-FDG PET/CT (Table 3).

In the grouping made according to the T stage, MTV (40% threshold) and ADC_{max} were significantly higher in T4 lesions than in T1-3 patients ($p=0.020$ and 0.007, respectively; Table 4). Based on these findings, ROC analysis was conducted for the MTV (40% threshold) and T stage (Figure 2).

No significant differences were identified in the analyzed parameters between low- and high-grade tumors (Table 5).

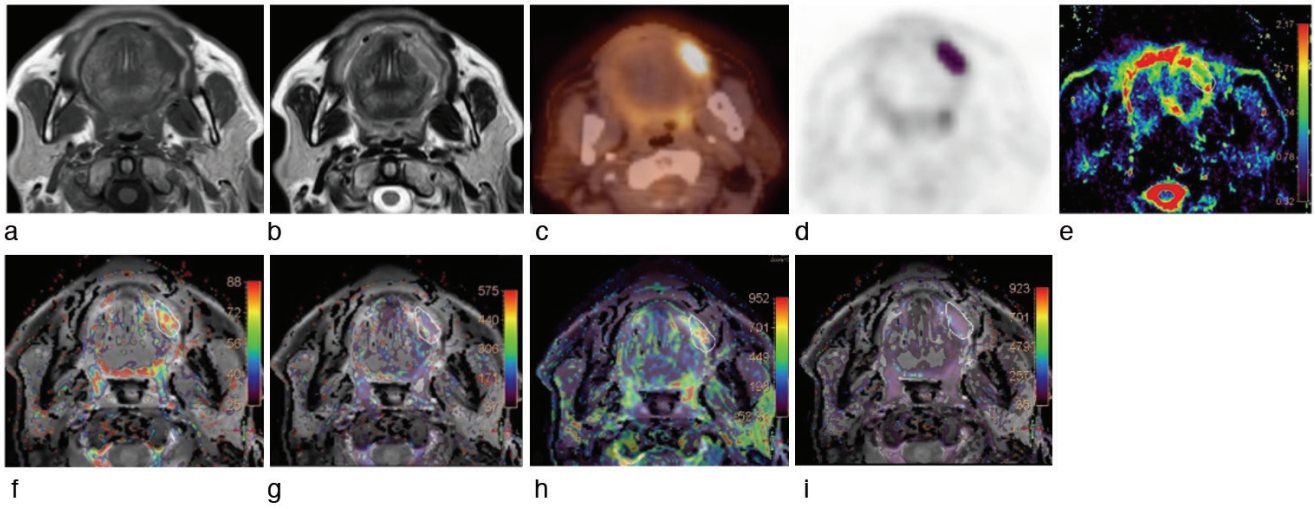


Figure 1. Imaging findings in a 61-year-old man with squamous cell carcinoma of the tongue ($T_2N_1M_0$). (a, b, c) T1- and T2-weighted images and ^{18}fluorine-fluorodeoxyglucose imaging (fused image) show left-sided tongue lesion [maximum standard uptake value (SUV_{max}): 10.2; SUV_{mean}: 5.3]. (d) Showing attenuation-corrected positron emission tomography image in LIFEx. (e) ADC map. The ADC values ($\times10^{-3}$ mm^2s^{-1}) of the lesion are as follows: ADC_{min}: 0.2, ADC_{mean}: 1.07, and ADC_{max}: 1.9. (f, g, h, i) Dynamic contrast-enhanced (DCE) imaging findings. Estimated DCE parameters are as follows: (f) Ktrans: 58.7 ($\times10^{-3}$ min^{-1}), (g) Kep: 303.1 ($\times10^{-3}$ min^{-1}), (h) Ve: 193.7 ($\times10^{-3}$), (i) iAUC: 159.1
ADC: Apparent diffusion coefficient, iAUC: Initial area under the curve

Table 1. DCE-MRI, DWI, and PET parameters in all patients

	Mean ± SD	Median	Range
SUV_{max}	12.1±1.2	11.9	3.8-20.7
SUV_{mean}	5.9±0.4	6.3	3.0-8.8
MTV (40% threshold) (mL)	11.7±2.9	9.9	1.1-35.8
TLG (40% threshold) (SUV × mL)	76.2±20.3	62.9	3.3-247.0
MTV (SUV 2.5 threshold) (mL)	20.9±5.7	15.4	2.1-72.1
TLG (SUV 2.5 threshold) (SUV × mL)	138.0±40.0	77.2	6.3-482.1
Ktrans (min^{-1})	0.05±0.04	0.05	0.03-0.09
Kep (min^{-1})	0.40±0.09	0.35	0.02-1.43
Ve	0.29±0.01	0.16	0.050-1.85
iAUC	116.6±10.2	111.1	64.6-184.1
ADC_{max} (10^{-3} mm^2/s)	2.35±0.16	2.2	1.5-3.5
ADC_{min} (10^{-3} mm^2/s)	0.3±0.1	0.2	0.1-1.0
ADC_{mean} (10^{-3} mm^2/s)	1.17±0.1	1.1	1.0-1.4

SD: Standard deviation, SUV: Standard uptake value, MTV: Metabolic tumor volume, TLG: Total lesion glycolysis, iAUC: Initial area under the curve, ADC: Apparent diffusion coefficient, DCE-MRI: Dynamic contrast-enhanced magnetic resonance imaging, DWI: Diffusion-weighted imaging, PET: Positron emission tomography, max: Maximum, min: Minimum

Table 2. Correlations* of DCE-MRI and DWI parameters in all patients

	ADC_{max}	ADC_{min}	ADC_{mean}
Ktrans	r=0.180 p=0.537	r=0.101 p=0.737	r=0.062 p=0.834
Kep	r=0.202 p=0.488	r=0.103 p=0.726	r=-0.496 p=0.072
Ve	r=-0.035 p=0.905	r=-0.110 p=0.709	**r=0.566** **p=0.035**
iAUC	r=-0.154 p=0.599	r=-0.389 p=0.169	r=0.445 p=0.111

*Spearman's correlation. iAUC: Initial area under the curve, ADC: Apparent diffusion coefficient, DCE-MRI: Dynamic contrast-enhanced magnetic resonance imaging, DWI: Diffusion-weighted imaging, max: Maximum, min: Minimum

In the grouping made according to the N stage, no significant difference was found between the parameters evaluated (Table 6).

Discussion

This study demonstrated several significant associations between PET, DCE-MRI, and DWI parameters with indicating relationships between glucose metabolism, tumor cellular density, and microvessel permeability of HNSCC.

In HNSCC, glucose metabolism is positively associated with the sum of tumor cells and growth rate. Accordingly, an inverse correlation between SUV and ADC parameters is expectable. The results of previous studies on this

Table 3. Correlations* of MRI and PET parameters in all patients

	SUV_{max}	SUV_{mean}	MTV (40% threshold)	TLG (40% threshold)	MTV (SUV 2.5 threshold)	TLG (SUV 2.5 threshold)
Ktrans	**r=-0.626** **p=0.017**	r=-0.304 p=0. 291	r=-0.196 p=0.503	r=-0.323 p=0.260	r=-0.380 p=0.180	r=-0.407 p=0.149
Kep	r=0.156 p=0.594	r=0.350 p=0.220	r=0.240 p=0.409	r=0.279 p=0.334	r=0.253 p=0.383	r=0.257 p=0.375
Ve	r=-0.380 p=0.180	r=-0.423 p=0.132	r=-0.398 p=0.159	r=-0.455 p=0.102	r=-0.459 p=0.098	r=-0.455 p=0.102
iAUC	**r=-0.732** **p=0.003**	**r=-0.700** **p=0.005**	**r=-0.745** **p=0.002**	**r=-0.824** **p=0.000**	**r=-0.815** **p=0.000**	**r=-0.815** **p=0.000**
ADC_{max}	r=-0.101 p=0.731	r=0.003 p=0.791	r=0.246 p=0.396	r=0.143 p=0.626	r=0.176 p=0.547	r=0.150 p=0.610
ADC_{min}	r=0.160 p=0.584	r=0.296 p=0.305	r=-0.018 p=0.950	r=0.110 p=0.709	r=0.062 p=0.834	r=0.071 p=0.810
ADC_{mean}	**r=-0.526** **p=0.053**	r=-0.455 p=0.102	r=-0.390 p=0.168	r=-0.456 p=0.101	r=-0.454 p=0.103	r=-0.489 p=0.076

*Spearman's correlation. SUV: Standard uptake value, MTV: Metabolic tumor volume, TLG: Total lesion glycolysis, iAUC: Initial area under the curve, ADC: Apparent diffusion coefficient, MRI: Magnetic resonance imaging, PET: Positron emission tomography, max: Maximum, min: Minimum

relationship in the literature are contradictory. For example, Zhang et al. (25) analyzed PET/MRI images of 27 patients with hypopharynx SCC, and Fruehwald-Pallamar et al. (18) analyzed ^{18}F-FDG PET/CT and MR images of 31 patients with HNSCC, and they did not observe a correlation between SUV_{max} and ADC. But Zhang et al. (25) observed an inverse correlation between MTV and ADC_{mean}. The other two studies showed that ADC_{min} tended to inversely correlate with SUV_{max} (p=0.08) (3,26). Also, Nakajo et al. (16) observed a negative correlation between SUV_{max} and ADC (20). In our study, we observed a tendency to an inverse correlation between SUV_{max} and ADC_{mean}, but it was not statistically significant (p=0.053).

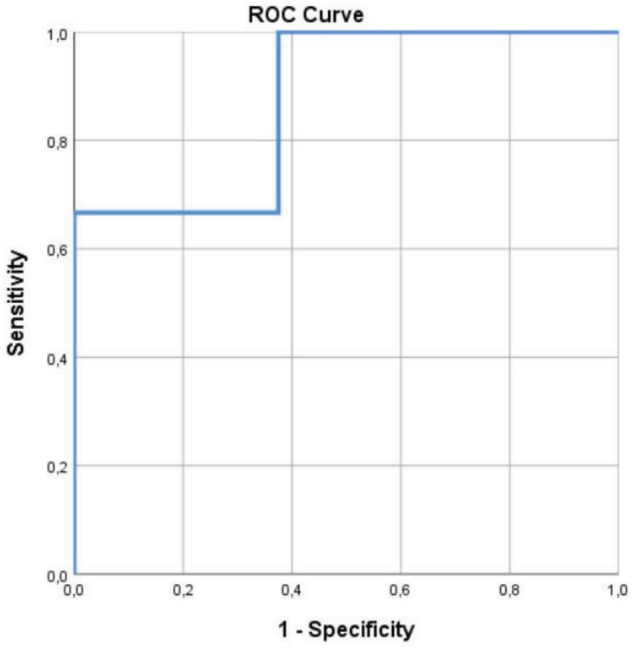


Figure 2. Receiver operating characteristics curves for advanced-stage tumor preliminary diagnosis of metabolic tumor volume (40% threshold) values. When we take the cut-off value as 5.4, the sensitivity is 100%, specificity is 62.5%, positive predictive value is 67%, negative predictive value is 100%, accuracy is 78.5%, area under curve is 0.875
ROC: Receiver operating characteristics

Many studies in the literature have investigated the relationship between T and N stages of tumors and PET parameters. Although Leifels et al. (3) did not observe significant differences in SUV_{max} between various T and N stages, Nakajo et al. (16) reported significantly higher SUV_{max} values in T3 and T4 tumors. In a previous study, T4 tumors had significantly higher SUV_{max} values than T1-3 tumors in patients with oral squamous cell carcinoma (27). In our study, we observed higher MTV (40% threshold) values in T4 tumors than T1-3 tumors. When we take the cut-off value as 5.4, the sensitivity, specificity, and AUC are 100%, 62.5%, and 0.875%, respectively. Because of the small number of patients, this cut-off value needs to be supported by studies with a higher number of patients to be more valuable. Also, TLG was higher in advanced-stage tumors but not statistically significant. T stage is determined according to the size and invasion characteristics of the tumor. As the tumor size increases, the number of tumor cells and, thus, the MTV increases. In HNSCC, T4 stage means that the tumor exceeds the limits of its primary focus and invades neighboring tissues. According to our results, MTV correlates with the tumoral invasion of adjacent tissues.

Many studies in the literature evaluated the relationship between T and N stages of the tumor and ADC values and found no significant differences (3,16,18). Zhang et al. (19) evaluated 541 cases with nasopharyngeal carcinoma, and the pretreatment ADC value in T3 and T4 tumors was significantly higher than in T1 and T2. In our study, ADC_{max}

Table 4. Comparison of PET, DCE-MRI, and DWI parameters between different T stages

Parameters	T1, T2, and T3 tumor Mean ± SD	T4 tumor Mean ± SD	p value*
SUV_{max}	11.2±4.8	13.3±4.5	0.519
SUV_{mean}	5.6±1.8	6.4±1.0	0.271
MTV (40% threshold)	6.0±4.7	19.4±12.4	**0.020**
TLG (40% threshold)	38.8±36.6	126.1±89.0	0.053
MTV (SUV 2.5 threshold)	10.3±8.9	35.0±25.7	0.053
TLG (SUV 2.5 threshold)	67.9±68.3	231.4±183.1	0.0.53
Ktrans	0.05±0.02	0.05±0.01	0.699
Kep	0.42±0.43	0.38±0.17	0.439
Ve	0.38±0.60	0.17±0.07	0.606
iAUC	126.8±45.6	102.9±21.8	0.245
ADC_{max}	2.03±0.38	2.79±0.54	**0.007**
ADC_{min}	0.386±0.3	0.213±0.2	0.179
ADC_{mean}	1.17±0.1	1.16±0.2	0.746

*Mann-Whitney U test. SUV: Standard uptake value, MTV: Metabolic tumor volume, TLG: Total lesion glycolysis, iAUC: Initial area under the curve, ADC: Apparent diffusion coefficient, PET: Positron emission tomography, DWI: Diffusion-weighted imaging, max: Maximum, min: Minimum

was significantly higher in T4 tumors than in T1-3 tumors. There was no significant difference in ADCmean and ADCmin values according to the T stage. Also, there was no significant difference in DCE, DWI, and PET parameters according to lymph node groups.

Correlations between DCE parameters and glucose metabolism and cellularity of the tumor were investigated in several studies (2,3,26). Leifel et al. (3) reported that Ktrans is significantly correlated with ADC_{max} and ADC_{mean} (3). Gawlitza et al. (26) observed a significant correlation between SUV_{mean} with Ktrans and Kep. Han et al. (2) did not observe a correlation between PET and DCE parameters. But in all three studies, a correlation was found between ADC_{mean} and Ve (p=0.0002, 0.06, and 0.000, respectively). In our research, in accordance with this result, a significant correlation was found between ADC mean and Ve (p=0.035). Ve is the indicator of EES. Accordingly, a high value of Ve implies that the number of cells in the tumor is low, which means less restricted water diffusion and, therefore, an increase in ADC value.

There are ambiguous associations described in the literature about the relationship between glucose metabolism and permeability. While one study demonstrated a correlation between SUV_{max} and Ktrans and between SUV_{mean} and Kep (26), others did not observe a correlation between perfusion and glucose metabolism parameters (2,3). In a study that involved 21 patients with advanced HCC, an inverse correlation was observed between Ktrans and SUV_{max} (28). Our results also showed an inverse correlation between Ktrans and SUV_{max}, indicating that HNSCC with higher glucose metabolism tends to have lower perfusion. This result

Table 5. Comparison of PET, DCE-MRI, and DWI parameters between low- and high-grade tumors

Parameters	Low grade Mean ± SD	High grade Mean ± SD	p value*
SUV_{max}	12.3±4.5	11.6±5.5	0.572
SUV_{mean}	5.8±1.2	6.2±2.3	0.777
MTV (40% threshold)	13.4±12.5	7.5±3.1	0.480
TLG (40% threshold)	86.5±87.1	50.4±32.2	0.671
MTV (SUV 2.5 threshold)	24.6±24.3	11.5±7.5	0.480
TLG (SUV 2.5 threshold)	161.7±169.7	78.7±66.0	0.671
Ktrans	0.05±0.01	0.06±0.02	0.120
Kep	0.39±0.39	0.44±0.12	0.322
Ve	0.34±0.54	0.16±0.09	0.572
iAUC	119.4±42.4	109.7±28.9	0.777
ADC_{max}	2.37±0.57	2.32±0.71	0.887
ADC_{min}	0.271±0.3	0.415±0.2	0.211
ADC_{mean}	1.15±0.1	1.21±0.2	0.723

*Mann-Whitney U test. SUV: Standard uptake value, MTV: Metabolic tumor volume, TLG: Total lesion glycolysis, iAUC: Initial area under the curve, ADC: Apparent diffusion coefficient, PET: Positron emission tomography, DCE-MRI: Dynamic contrast-enhanced magnetic resonance imaging, DWI: Diffusion-weighted imaging, max: Maximum, min: Minimum

Table 6. Comparison of PET, DCE-MRI, and DWI parameters between different tumor N stages

Parameters	Lymph node (-) Mean ± SD	Lymph node (+) Mean ± SD	p value*
SUV_{max}	10.5±3.6	13.3±5.2	0.245
SUV_{mean}	5.5±1.4	6.3±1.6	0.271
MTV (40% threshold)	10.9±12.9	12.3±10.1	0.439
TLG (40% threshold)	68.6±91.0	81.9±68.7	0.439
MTV (SUV 2.5 threshold)	16.8±18.6	24.0±24.1	0.606
TLG (SUV 2.5 threshold)	105.4±131.8	162.4±166.5	0.519
Ktrans	0.05±0.01	0.05±0.02	0.606
Kep	0.49±0.47	0.34±0.19	0.897
Ve	0.17±0.1	0.38±0.6	0.379
iAUC	123.0±38.7	111.8±39.7	0.439
ADC_{max}	2.23±0.33	2.44±0.73	0.747
ADC_{min}	0.308±0.35	0.312±0.27	0.545
ADC_{mean}	1.15±0.12	1.18±0.16	0.605

*Mann-Whitney U test. SUV: Standard uptake value, MTV: Metabolic tumor volume, TLG: Total lesion glycolysis, iAUC: Initial area under the curve, ADC: Apparent diffusion coefficient, PET: Positron emission tomography, DCE-MRI: Dynamic contrast-enhanced magnetic resonance imaging, DWI: Diffusion-weighted imaging, max: Maximum, min: Minimum

is contrary to the understanding that the increase in the grade would increase perfusion. In the early stage, tumor growth and vascularization are proportional. In contrast, the increase in tumor growth is faster than the increase in vascularity in the later stages, which can cause insufficient perfusion and necrosis (28,29). However, Surov et al. (30), observed a correlation between SUV_{max} and microvessel density in HNSCC. So, our results need to be supported by other studies.

This study also showed that iAUC was inversely correlated with SUV_{max}, SUV_{mean}, MTV, and TLG. Zhang et al. (31) found an inverse correlation between SUV_{mean} and iAUC in their study, in which they evaluated PET/CT and DCE-MRI images of 41 non-small cell lung cancer patients. Bisdas et al. (32) analyzed this relation in 27 patients with head and neck cancer and identified that iAUC correlated with SUV_{max} and SUV_{mean}. iAUC refers to the amount of contrast agent that reaches and retains the tumor tissue at particular time (32). iAUC is a semi-quantitative parameter of DCE- MRI. So, evaluating the correlation of iAUC with other quantitative parameters has some difficulties. It can be affected by changes in physiological conditions and differences in sequence duration (26). Cheng (33) stated that conventional iAUC could not be an alternative for quantitative parameters such as Ktrans and Kep. Still, if it becomes precise and reproducible with new methods, it can be their alternative. Considering all these, the interpretation of the inverse correlation between the iAUC and PET parameters obtained in this study will not be clear; thus, further studies are needed on this subject.

In this study, no significant association was found between tumor grade and any imaging parameters as in another study (3). Haerle et al. (6) evaluated PET/CT images of 262 patients with HNSCC and did not show a correlation between SUV_{max} and tumor grade. Choi et al. (34) and Nakajo et al. (16) also found no association between SUV_{max} and ADC with grade. Zheng et al. (27) analyzed 104 patients with oral SCC and observed an association between SUV_{max} and poor differentiation. Different grading systems in HNSCC include parameters such as lymphoplasmacytic infiltration, keratinization degree of the tumor, nuclear and cellular polymorphism, and invasion pattern (35). However, parameters such as tumor cellularity, glucose metabolism, microvessel density, and EES that were evaluated with imaging methods in this study were not considered (3). Both the small number of patients in the high-grade group (n=4) and these reasons may explain the absence of a relationship between grade and imaging parameters in our study.

Study Limitations

The most important limitations of this study are its retrospective design and the small number of patients. Additionally, the DWI and DCE parameters were obtained from freehand ROIs, whereas the PET parameters were obtained from a certain threshold automatically, and this may lead to inaccuracies to some degree. Only pretreatment imaging and histopathology data of the patients were evaluated. Therefore, their potential role in predicting treatment response or relapse has not been evaluated. In this study, all HNSCC tumors were included, and differences may arise due to different tumor localizations that were ignored.

Conclusion

We analyzed the relationships among imaging parameters derived from DCE-MRI, DWI, and ^{18}F-FDG PET/CT to reveal the complex biological structure of HNSCC with multiparametric functional imaging methods. We observed significant associations among these parameters at different degrees. MTV (40% threshold) was useful for predicting T4 tumors. Further studies are necessary to prove these results and investigate the possible complementary contribution of these techniques on explaining HNSCC characteristics.

Ethics

Ethics Committee Approval: Dokuz Eylül University Institutional Ethics Board approved this study (file number: 5538-GOA).

Informed Consent: The necessity for written informed consent was waived.

Peer-review: Externally peer-reviewed.

Surgical and Medical Practices: H.M.B., O.B., S.S., Ö.Ö., E.D., N.K., Concept: H.M.B., O.B., S.S., Ö.Ö., E.D., N.K., Design: H.M.B., O.B., S.S., Ö.Ö., E.D., N.K., Data Collection or Processing: H.M.B., O.B., S.S., Ö.Ö., E.D., N.K., Analysis or Interpretation: H.M.B., O.B., S.S., Ö.Ö., E.D., N.K., Literature Search: H.M.B., O.B., S.S., Ö.Ö., E.D., N.K., Writing: H.M.B., O.B., S.S., Ö.Ö., E.D., N.K.

Conflict of Interest: No conflict of interest was declared by the authors.

Financial Disclosure: The authors declared that this study has received no financial support.

References

1. Covello M, Cavaliere C, Aiello M, Cianelli MS, Mesolella M, Iorio B, Rossi A, Nicolai E. Simultaneous PET/MR head-neck cancer imaging: Preliminary clinical experience and multiparametric evaluation. Eur J Radiol 2015;84:1269-1276.
2. Han M, Kim SY, Lee SJ, Choi JW. The Correlations Between MRI Perfusion, Diffusion Parameters, and 18F-FDG PET Metabolic Parameters in Primary

Head-and-Neck Cancer: A Cross-Sectional Analysis in Single Institute. Medicine (Baltimore) 2015;94:e2141.

3. Leifels L, Purz S, Stumpp P, Schob S, Meyer HJ, Kahn T, Sabri O, Surov A. Associations between 18F-FDG-PET, DWI, and DCE Parameters in Patients with Head and Neck Squamous Cell Carcinoma Depend on Tumor Grading. Contrast Media Mol Imaging 2017;2017:5369625.
4. Ong SC, Schöder H, Lee NY, Patel SG, Carlson D, Fury M, Pfister DG, Shah JP, Larson SM, Kraus DH. Clinical utility of 18F-FDG PET/CT in assessing the neck after concurrent chemoradiotherapy for Locoregional advanced head and neck cancer. J Nucl Med 2008;49:532-540.
5. Surov A, Meyer HJ, Höhn AK, Sabri O, Purz S. Combined Metabolo-Volumetric Parameters of 18F-FDG-PET and MRI Can Predict Tumor Cellularity, Ki67 Level and Expression of HIF 1alpha in Head and Neck Squamous Cell Carcinoma: A Pilot Study. Transl Oncol 2019;12:8-14.
6. Haerle SK, Huber GF, Hany TF, Ahmad N, Schmid DT. Is there a correlation between 18F-FDG-PET standardized uptake value, T-classification, histological grading and the anatomic subsites in newly diagnosed squamous cell carcinoma of the head and neck? Eur Arch Otorhinolaryngol 2010;267:1635-1640.
7. Pak K, Cheon GJ, Nam HY, Kim SJ, Kang KW, Chung JK, Kim EE, Lee DS. Prognostic value of metabolic tumor volume and total lesion glycolysis in head and neck cancer: a systematic review and meta-analysis. J Nucl Med 2014;55:884-890.
8. Im HJ, Pak K, Cheon GJ, Kang KW, Kim SJ, Kim IJ, Chung JK, Kim EE, Lee DS. Prognostic value of volumetric parameters of (18)F-FDG PET in non-small-cell lung cancer: a meta-analysis. Eur J Nucl Med Mol Imaging 2015;42:241-251.
9. Im HJ, Kim YK, Kim YI, Lee JJ, Lee WW, Kim SE. Usefulness of Combined Metabolic-Volumetric Indices of (18)F-FDG PET/CT for the Early Prediction of Neoadjuvant Chemotherapy Outcomes in Breast Cancer. Nucl Med Mol Imaging 2013;47:36-43.
10. Burger IA, Casanova R, Steiger S, Husmann L, Stolzmann P, Huellner MW, Curioni A, Hillinger S, Schmidtlein CR, Soltermann A. 18F-FDG PET/CT of Non-Small Cell Lung Carcinoma Under Neoadjuvant Chemotherapy: Background-Based Adaptive-Volume Metrics Outperform TLG and MTV in Predicting Histopathologic Response. J Nucl Med 2016;57:849-854.
11. Im HJ, Kim TS, Park SY, Min HS, Kim JH, Kang HG, Park SE, Kwon MM, Yoon JH, Park HJ, Kim SK, Park BK. Prediction of tumour necrosis fractions using metabolic and volumetric 18F-FDG PET/CT indices, after one course and at the completion of neoadjuvant chemotherapy, in children and young adults with osteosarcoma. Eur J Nucl Med Mol Imaging 2012;39:39-49.
12. Bernstein JM, Homer JJ, West CM. Dynamic contrast-enhanced magnetic resonance imaging biomarkers in head and neck cancer: potential to guide treatment? A systematic review. Oral Oncol 2014;50:963-970.
13. Surov A, Meyer HJ, Wienke A. Correlation between apparent diffusion coefficient (ADC) and cellularity is different in several tumors: a meta-analysis. Oncotarget 2017;8:59492-59499.
14. Shukla-Dave A, Lee NY, Jansen JF, Thaler HT, Stambuk HE, Fury MG, Patel SG, Moreira AL, Sherman E, Karimi S, Wang Y, Kraus D, Shah JP, Pfister DG, Koutcher JA. Dynamic contrast-enhanced magnetic resonance imaging as a predictor of outcome in head-and-neck squamous cell carcinoma patients with nodal metastases. Int J Radiat Oncol Biol Phys 2012;82:1837-1844.
15. Meyer HJ, Purz S, Sabri O, Surov A. Relationships between histogram analysis of ADC values and complex 18F-FDG-PET parameters in head and neck squamous cell carcinoma. PLoS One 2018;13:e0202897.
16. Nakajo M, Nakajo M, Kajiya Y, Tani A, Kamiyama T, Yonekura R, Fukukura Y, Matsuzaki T, Nishimoto K, Nomoto M, Koriyama C. FDG PET/CT and diffusion-weighted imaging of head and neck squamous cell carcinoma: comparison of prognostic significance between primary tumor standardized uptake value and apparent diffusion coefficient. Clin Nucl Med 2012;37:475-480.
17. Varoquaux A, Rager O, Lovblad KO, Masterson K, Dulguerov P, Ratib O, Becker CD, Becker M. Functional imaging of head and neck squamous cell carcinoma with diffusion-weighted MRI and FDG PET/CT: quantitative analysis of ADC and SUV. Eur J Nucl Med Mol Imaging 2013;40:842-852.
18. Fruehwald-Pallamar J, Czerny C, Mayerhoefer ME, Halpern BS, Eder-Czembirek C, Brunner M, Schuetz M, Weber M, Fruehwald L, Herneth AM. Functional imaging in head and neck squamous cell carcinoma: correlation of PET/CT and diffusion-weighted imaging at 3 Tesla. Eur J Nucl Med Mol Imaging 2011;38:1009-1019.
19. Zhang Y, Liu X, Zhang Y, Li WF, Chen L, Mao YP, Shen JX, Zhang F, Peng H, Liu Q, Sun Y, Ma J. Prognostic value of the primary lesion apparent diffusion coefficient (ADC) in nasopharyngeal carcinoma: a retrospective study of 541 cases. Sci Rep 2015;5:12242.
20. Martens RM, Noij DP, Koopman T, Zwezerijnen B, Heymans M, de Jong MC, Hoekstra OS, Vergeer MR, de Bree R, Leemans CR, de Graaf P, Boellaard R, Castelijns JA. Predictive value of quantitative diffusion-weighted imaging and 18-F-FDG-PET in head and neck squamous cell carcinoma treated by (chemo)radiotherapy. Eur J Radiol 2019;113:39-50.
21. Gaddikeri S, Gaddikeri RS, Tailor T, Anzai Y. Dynamic Contrast-Enhanced MR Imaging in Head and Neck Cancer: Techniques and Clinical Applications. AJNR Am J Neuroradiol 2016;37:588-595.
22. Nioche C, Orlhac F, Boughdad S, Reuzé S, Goya-Outi J, Robert C, Pellot-Barakat C, Soussan M, Frouin F, Buvat I. LIFEx: A Freeware for Radiomic Feature Calculation in Multimodality Imaging to Accelerate Advances in the Characterization of Tumor Heterogeneity. Cancer Res 2018;78:4786-4789.
23. Im HJ, Bradshaw T, Solaiyappan M, Cho SY. Current Methods to Define Metabolic Tumor Volume in Positron Emission Tomography: Which One is Better? Nucl Med Mol Imaging 2018;52:5-15.
24. Fonti R, Larobina M, Del Vecchio S, De Luca S, Fabbricini R, Catalano L, Pane F, Salvatore M, Pace L. Metabolic tumor volume assessed by 18F-FDG PET/CT for the prediction of outcome in patients with multiple myeloma. J Nucl Med 2012;53:1829-1835.
25. Zhang L, Song T, Meng Z, Huang C, Chen X, Lu J, Xian J. Correlation between apparent diffusion coefficients and metabolic parameters in hypopharyngeal squamous cell carcinoma: a prospective study with integrated PET/MRI. Eur J Radiol 2020;129:109070.
26. Gawlitza M, Purz S, Kubiessa K, Boehm A, Barthel H, Kluge R, Kahn T, Sabri O, Stumpp P. In Vivo Correlation of Glucose Metabolism, Cell Density and Microcirculatory Parameters in Patients with Head and Neck Cancer: Initial Results Using Simultaneous PET/MRI. PLoS One 2015;10:e0134749.
27. Zheng D, Niu L, Liu W, Zheng C, Yan R, Gong L, Dong Z, Li K, Fei J. Correlation analysis between the SUVmax of FDG-PET/CT and clinicopathological characteristics in oral squamous cell carcinoma. Dentomaxillofac Radiol 2019;48:20180416.
28. Ahn SJ, Park MS, Kim KA, Park JY, Kim I, Kang WJ, Lee SK, Kim MJ. ^{18}F-FDG PET metabolic parameters and MRI perfusion and diffusion parameters in hepatocellular carcinoma: a preliminary study. PLoS One 2013;8:e71571.
29. Strosberg JR, Coppola D, Klimstra DS, Phan AT, Kulke MH, Wiseman GA, Kvols LK; North American Neuroendocrine Tumor Society (NANETS). The NANETS consensus guidelines for the diagnosis and management of poorly differentiated (high-grade) extrapulmonary neuroendocrine carcinomas. Pancreas 2010;39:799-800.
30. Surov A, Meyer HJ, Höhn AK, Wienke A, Sabri O, Purz S. 18F-FDG-PET Can Predict Microvessel Density in Head and Neck Squamous Cell Carcinoma. Cancers (Basel) 2019;11:543.
31. Zhang J, Chen L, Chen Y, Wang W, Cheng L, Zhou X, Wang J. Tumor vascularity and glucose metabolism correlated in adenocarcinoma, but not in squamous cell carcinoma of the lung. PLoS One 2014;9:e91649.
32. Bisdas S, Seitz O, Middendorp M, Chambron-Pinho N, Bisdas T, Vogl TJ, Hammerstingl R, Ernemann U, Mack MG. An exploratory pilot study into

the association between microcirculatory parameters derived by MRI-based pharmacokinetic analysis and glucose utilization estimated by PET-CT imaging in head and neck cancer. Eur Radiol 2010;20:2358-2366.

33. Cheng HL. Investigation and optimization of parameter accuracy in dynamic contrast-enhanced MRI. J Magn Reson Imaging 2008;28:736-743.
34. Choi SH, Paeng JC, Sohn CH, Pagsisihan JR, Kim YJ, Kim KG, Jang JY, Yun TJ, Kim JH, Han MH, Chang KH. Correlation of 18F-FDG uptake with apparent diffusion coefficient ratio measured on standard and high b value diffusion MRI in head and neck cancer. J Nucl Med 2011;52:1056-1062.
35. Sawazaki-Calone I, Rangel A, Bueno AG, Morais CF, Nagai HM, Kunz RP, Souza RL, Rutkauskis L, Salo T, Almangush A, Coletta RD. The prognostic value of histopathological grading systems in oral squamous cell carcinomas. Oral Dis 2015;21:755-761.